Joint Delay and Doppler Estimation for Passive Sensing With Direct-Path Interference

Xin Zhang, Hongbin Li, *Senior Member, IEEE*, Jun Liu, *Member, IEEE*, and Braham Himed, *Fellow, IEEE*

***Abstract*—We consider the problem of joint delay-Doppler estimation of a moving target in a passive radar that employs a non-cooperative illuminator of opportunity (IO) for target illumination, a reference channel (RC) steered to the IO to obtain a reference signal, and a surveillance channel (SC) for target monitoring. We consider a practically motivated scenario, where the RC receives a noise-contaminated copy of the IO signal and the SC observation is polluted by a direct-path interference that is usually neglected by prior studies. We develop a data model without discretizing the parameter space, which may lead to a straddle loss, by treating both the delay and Doppler as continuous parameters. We propose an expectation-maximization based estimator, as well as a modified cross-correlation (MCC) estimator that is a computationally simpler solution resulting from an approximation of the former. In addition, we derive the Cramér-Rao lower bound for the estimation problem. Simulation results are presented to illustrate the performance of the proposed estimators and the widely used CC estimator.**

***Index Terms*—Direct-path interference, joint delay-Doppler estimation, noisy reference, passive sensing.**

I. Introduction

PASSIVE sensing is employed in many applications, such as radar, underwater acoustics, seismology, and many others [1]–[7]. A passive radar system, which detects and tracks targets of interest by utilizing non-cooperative illuminators of opportunity (IOs) [1]–[5], has a number of benefits compared with its active counterpart. First, since a transmitter is not required, a passive radar is smaller and less expensive. Second, by using ambient communication signals, such as radio and television broadcasting signals [3], [4], a passive radar has the ability to operate in a wide frequency band without causing interference to existing wireless systems. Finally, spatial diversity can be readily exploited for improved target detection and classification capabilities through bistatic or multistatic configuration of a passive radar system [8].

Manuscript received May 05, 2015; revised August 27, 2015; accepted September 24, 2015. Date of publication October 08, 2015; date of current version January 05, 2016. The associate editor coordinating the review of this manuscript and approving it for publication was Dr. Joseph Guerci.

X. Zhang and H. Li are with the Department of Electrical and Computer Engineering, Stevens Institute of Technology, Hoboken, NJ 07030 USA (e-mail: xzhang23@stevens.edu; Hongbin.Li@stevens.edu).

J. Liu was with the Department of Electrical and Computer Engineering, Stevens Institute of Technology, Hoboken, NJ 07030 USA. He is now with the National Laboratory of Radar Signal Processing, Xidian University, Xi'an, 710071, China (e-mail: jun_liu_math@hotmail.com).

B. Himed is with the AFRL/RYMD, Dayton, OH 45433 USA (e-mail: braham.himed@us.af.mil).

Color versions of one or more of the figures in this paper are available online at http://ieeexplore.ieee.org.

Digital Object Identifier 10.1109/TSP.2015.2488584

Since the transmitted signal is unknown due to the non-cooperative nature of the IO, a passive radar often utilizes a reference channel (RC) at the receiver to collect a direct-path (transmitter-to-receiver) signal and, respectively, a surveillance channel (SC) to measure a potential target echo [1]–[4]. An RC is usually implemented by using directional antennas [9]. Given both the RC and SC observations, a cross-correlation (CC) operation can be conducted between the two channels to mimic matched filtering (MF) in active radar, where the reference signal obtained with the RC plays the role of the transmitted signal in the MF operation. However, the CC operation is sub-optimal, because the reference signal is contaminated by the inevitable channel noise in the RC. In [10], [11], the effect of noise in the RC is taken into account, and several improved passive detectors are developed by treating the transmitted waveform as a deterministic or random process. The effect of noise is also examined in [12] in a passive multi-input multi-output (MIMO) radar setup, where the interplay between the noise in the RC and the noise in the SC is extensively studied. Instead of using a dedicated RC to measure the transmitted signal, an alternative approach to passive sensing is to employ multi-channel observations (e.g., via an antenna array) of the target echo and exploit the inter-channel correlations for target estimation and detection [13]–[16]. Sometimes, the transmitted signal may exhibit certain modulation induced structures that can be exploited for passive sensing without using a dedicated RC as well. For example, the P1 symbol embedded in the second generation digital video broadcasting-terrestrial (DVB-T2) signals is employed for target detection in [17] and [18].

Nevertheless, there exist some issues in the above studies. One limitation is that either the target parameters (propagation delay and Doppler shift) are assumed known, or a scanning process is involved in the detection process, where the two-dimensional delay-Doppler uncertainty region is discretized into small cells and the detection is performed on each cell in a sequential fashion (e.g., [10]–[16]). Such discretization may lead to a straddle loss and degraded detection performance. Another limitation with the previous studies is that they often assume the SC only receives the target echo but not the direct-path signal from the transmitter. In practice, while the direct-path signal is mitigated by, e.g., a directional antenna, some residual, henceforth referred to as the *direct-path interference* (DPI), may still exist in the SC. In particular, the direct-path signal is generally much stronger (by many tens of dB) compared with the target echo [19]. Non-negligible DPI may be caused by possible mismatches between the null of the antenna and the direction of arrival of the DPI due to, e.g., vibrations of the radar platform

[20]. Furthermore, when an adaptive antenna array is used to mitigate the DPI [20], [21], the mitigation is limited by the array size which dictates the null depth. As a result, the DPI in the SC may still be at a power level comparable to the target echo.

We examine herein the joint delay-Doppler estimation problem for passive sensing by using observations from an RC and SC. We consider the case when both channels are contaminated by non-negligible disturbance and, in addition, the DPI is present in the SC. The problem involves estimating the delay and Doppler of the target and other related parameters including the transmitted waveform and the channel coefficients of the SC. Unlike conventional methods (e.g., the aforementioned scanning based solutions) that discretize the parameter space and may lead to a straddle loss, we develop a data model which treats both the delay and Doppler as continuous parameters without discretization. As the problem is highly non-linear, we develop an iterative estimation algorithm based on the expectation-maximization (EM) principle [22], along with several simplifications aimed at improving the computational efficiency. Analysis is provided to shed light on the problem, which reveals that the proposed algorithm consists of iterations of sequential DPI cancellation and data fitting. Based on this insight, we introduce a modified CC estimator, which is computationally more efficient, involving a single DPI cancellation followed by cross-correlation. In addition, we derive the Cramér-Rao lower bound (CRLB) for the estimation problem to benchmark the proposed estimators.

The remainder of the paper is organized as follows. In Section II, we formulate the passive radar system model. In Section III, the proposed approaches and the CRLB are derived. Numerical results and discussions are included in Section IV, followed by conclusions in Section V.

Notation: Vectors (matrices) are denoted by boldface lower (upper) case letters, and all vectors are column vectors. Superscripts $(\cdot)^*$, $(\cdot)^T$, and $(\cdot)^H$ denote complex conjugate, transpose, and complex conjugate transpose, respectively. $\Re\{\cdot\}$ represents the real part of a complex quantity and $E\{\cdot\}$ denotes statistical expectation. $\mathbf{0}_{p\times q}$ denotes a $p\times q$ matrix with all zero entries, $\mathbf{I}_n$ denotes an identity matrix of size n, $\odot$ stands for the Hadamard product, $[\cdot]_{m,n}$ denotes an entry at the m-th row and the n-th column of a matrix, and $[\cdot]_m$ denotes the m-th element of a vector. $\mathcal{CN}$ denotes a circularly symmetric, complex Gaussian $\det(\cdot)$ represents the determinant of a matrix, $\|\cdot\|$ is the Frobenius norm, and $\mathrm{tr}\{\cdot\}$ denotes the trace of a matrix.

II. System Model

Consider a scenario depicted in Fig. 1, where a passive radar employs a non-cooperative illuminator of opportunity (IO) for moving target detection and estimation. The passive radar is equipped with an RC to receive the unknown source signal sent directly from the IO, as well as an SC to observe the target echo. A directional antenna is utilized at the passive radar receiver to form the RC, with its main-beam pointing to the IO. Then, the signal received in the RC can be written as

$$y_r'(t) = \gamma x'(t - t_r) + n_r'(t), \tag{1}$$

where $x'(t)$ is the unknown signal (baseband equivalent) transmitted by the IO, γ is the scaling coefficient accounting for the antenna gain and the channel propagation effects from the IO to the RC, t_r is the propagation delay between the IO and the RC, and $n_r'(t)$ is the additive zero-mean Gaussian disturbance (clutter and noise) in the RC.

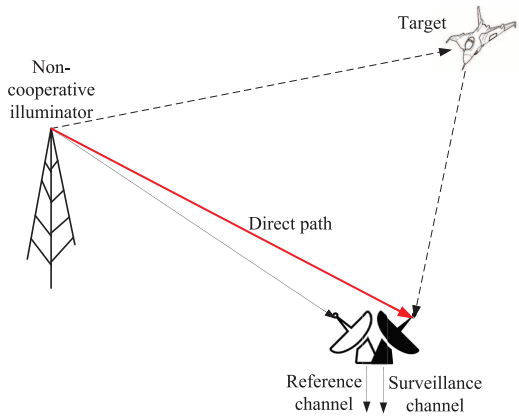

Fig. 1. A passive radar system with a reference channel and surveillance channel.

For the SC, a different antenna or antenna beam is used to receive the target echo. Although it is standard for the SC to employ some DPI suppression scheme, there may still exist non-negligible DPI as noted before. The signal received in the SC can be expressed as

$$y_s'(t) = \beta' x'(t - t_r) + \alpha' x'(t - t_s) e^{j2\pi f_d t} + n_s'(t), \tag{2}$$

where β' is the scaling coefficient considering the antenna attenuation and the channel propagation effects from the IO to the SC, t_r is the propagation delay of the DPI, which is identical to that in (1) since the RC and SC are co-located, α' is the scaling coefficient accounting for the target reflectivity, the antenna gain, and the channel propagation effects, t_s is the propagation delay due to the transmission from the IO to the target and then from the target to the SC, f_d is the Doppler frequency, and $n_s'(t)$ is the additive zero-mean Gaussian disturbance (clutter and noise) in the SC.

To simplify our system model, it is observed that the bistatic delay $\tau = t_s - t_r$ is of interest in practice, and the direct-path delay t_r is generally known a priori since the location of the IO is usually known. Thus, we can compensate for the delay t_r in the received signals. Moreover, since γ and $x'(t)$ are both unknown, they cannot be separately estimated. In the sequel, γ is absorbed into $x'(t)$. Define the delay-compensated signals as $y_r(t) = y_r'(t + t_r)$ and $y_s(t) = y_s'(t + t_r)$. The delay-compensated disturbances $n_r(t)$ and $n_s(t)$ are similarly defined. Accordingly, the system model in the time domain can be formulated into a compact form:

$$\begin{aligned} y_r(t) &= x(t) + n_r(t), \\ y_s(t) &= \beta x(t) + \alpha x(t - \tau) e^{j2\pi f_d t} + n_s(t), \end{aligned} \tag{3}$$

where $x(t) = \gamma x'(t)$, $\beta = \beta'/\gamma$, and $\alpha = \alpha' e^{j2\pi f_d t_r}/\gamma$. Note that our system model is notably different from those in prior delay-Doppler estimation works (e.g., [23]–[26]), due to the different application targeted herein, namely, the 2-channel passive sensing problem with DPI.

We assume that $x(t)$ has a duration of T seconds, e.g., due to the framed transmissions employed by the IO, in which case T represents the frame duration. The observation interval T_o is selected such that $T_o \geq T + \tau_{\max}$, where $\tau_{\max}$ denotes the maximum bistatic delay of the passive radar system. We sample the RC and the SC signals using a sampling frequency $f_s \geq 2(B + f_{\max})$, where B denotes the bandwidth of the communication signal $x(t)$ and $f_{\max}$ is the maximum Doppler frequency of the target that is designed detectable by the passive radar. Suppose M samples are collected over the observation window T_o, i.e., $T_o = MT_s$ where $T_s = 1/f_s$ denotes the sampling interval. Let $\bar{\mathbf{y}}_r = [y_r(0), y_r(T_s), \ldots, y_r((M-1)T_s)]^T$, $\bar{\mathbf{x}}_d(\tau) = [x(0-\tau), x(T_s-\tau), \ldots, x((M-1)T_s-\tau)]^T$[1] and $\bar{\mathbf{y}}_s$, $\bar{\mathbf{x}}$, $\bar{\mathbf{n}}_r$, and $\bar{\mathbf{n}}_s$ be similarly defined $M \times 1$ vectors formed from samples of $y_s(t)$, $x(t)$, $n_r(t)$, and $n_s(t)$, respectively. The digitized model becomes

$$\begin{cases} \bar{\mathbf{y}}_r = \bar{\mathbf{x}} + \bar{\mathbf{n}}_r \\ \bar{\mathbf{y}}_s = \beta\bar{\mathbf{x}} + \alpha\bar{\mathbf{x}}_d(\tau) \odot \bar{\mathbf{a}}(f_d) + \bar{\mathbf{n}}_s \end{cases}, \tag{4}$$

where

$$\bar{\mathbf{a}}(f_d) = [1, e^{j2\pi f_d T_s}, \ldots, e^{j2\pi f_d (M-1)T_s}]^T. \tag{5}$$

In this work, we assume $\bar{\mathbf{x}}$, $\bar{\mathbf{n}}_r$, and $\bar{\mathbf{n}}_s$ are zero-mean Gaussian distributed with covariance matrices $\mathbf{R}_x$, $\mathbf{R}_{nr}$, and $\mathbf{R}_{ns}$, respectively. In particular, it is noted that the signal waveform is modeled as a correlated stochastic process. This stochastic model is suitable for the IOs using orthogonal frequency division multiplexing (OFDM) based modulations, which involve multiple random information streams riding on different subcarriers to form a composite transmitted signal and can be well appropriated as Gaussian by the central limit theorem [11]. OFDM based modulations are popular choices for broadband wireless systems including the DVB-T2.

Denote the M-point discrete Fourier transform (DFT) of $\bar{\mathbf{y}}_r$ as $\mathbf{y}_r = \mathbf{T}\bar{\mathbf{y}}_r$, where the DFT matrix $\mathbf{T}$ has the entries $[\mathbf{T}]_{p,q} = e^{-j2\pi(p-1)\Delta f(q-1)T_s}/\sqrt{M}$, $p, q = 1, 2, \ldots, M$, with the frequency spacing $\Delta f = \frac{f_s}{M} = \frac{1}{T_s M}$, and $\mathbf{y}_s$, $\mathbf{x}$, $\mathbf{n}_r$, $\mathbf{n}_s$, $\mathbf{a}(f_d)$ are similarly defined $M \times 1$ vectors. Let

$$\mathbf{a}(f_d) = [A(0), A(\Delta f), \ldots, A((M-1)\Delta f)]^T, \tag{6}$$

where

$$A(m\Delta f) = \begin{cases} \sqrt{M}, & \text{if } m = \frac{f_d}{\Delta f} \\ \dfrac{1 - e^{j2\pi\left(\frac{f_d}{\Delta f} - m\right)}}{\sqrt{M}\left[1 - e^{j\frac{2\pi}{M}\left(\frac{f_d}{\Delta f} - m\right)}\right]}, & \text{otherwise} \end{cases} \tag{7}$$

for $m = 0, 1, \ldots, M-1$. Applying basic DFT properties [27], we can write the system model in the frequency domain as

$$\begin{cases} \mathbf{y}_r = \mathbf{x} + \mathbf{n}_r \\ \mathbf{y}_s = \beta\mathbf{x} + \alpha\mathbf{A}(f_d)\mathbf{W}(\tau)\mathbf{x} + \mathbf{n}_s \end{cases}, \tag{8}$$

where $\mathbf{A}(f_d)$ is a circulant matrix formed from $\mathbf{a}(f_d)$ and $\mathbf{W}(\tau)$ is a diagonal matrix with diagonal entries $[\mathbf{W}(\tau)]_{p,p} = e^{-j2\pi\Delta f(p-1)\tau}$, $p = 1, 2, \ldots, M$. Since the sequence $\{A(m\Delta f)\}$ is periodic with period M, we have $A((M-m)\Delta f) = A((-m)\Delta f)$. Hence, the matrix $\mathbf{A}(f_d)$ is

$$[\mathbf{A}(f_d)]_{p,q} = \frac{1}{\sqrt{M}} A((p-q)\Delta f),\ p, q = 1, 2, \ldots, M. \tag{9}$$

Clearly, $\mathbf{x}$, $\mathbf{n}_r$, and $\mathbf{n}_s$ are Gaussian random vectors with zero mean and covariance matrices $\mathbf{C}_x = \mathbf{T}\mathbf{R}_x\mathbf{T}^H$, $\mathbf{C}_{nr} = \mathbf{T}\mathbf{R}_{nr}\mathbf{T}^H$, and $\mathbf{C}_{ns} = \mathbf{T}\mathbf{R}_{ns}\mathbf{T}^H$. It is assumed that the vectors $\mathbf{x}$, $\mathbf{n}_r$, $\mathbf{n}_s$ are mutually independent and their covariance matrices $\mathbf{C}_x$, $\mathbf{C}_{nr}$, $\mathbf{C}_{ns}$ are known. In practice, the covariance matrices can be estimated by exploiting training data [28].

The problem of interest is to jointly estimate the unknown parameters β, α, τ, and f_d from the observations $\mathbf{y}_r$ and $\mathbf{y}_s$. In the following, the arguments in the matrices $\mathbf{A}(f_d)$ and $\mathbf{W}(\tau)$ are dropped for simplicity.

III. Proposed Approaches

Let $\mathbf{y} = [\mathbf{y}_r^T, \mathbf{y}_s^T]^T$. Clearly, $\mathbf{y}$ is Gaussian with zero mean and covariance matrix

$$\mathbf{C}_y = E\{\mathbf{y}\mathbf{y}^H\} = \begin{bmatrix} \mathbf{G} & \mathbf{B} \\ \mathbf{B}^H & \mathbf{D} \end{bmatrix}, \tag{10}$$

where

$$\mathbf{G} = \mathbf{C}_x + \mathbf{C}_{nr}, \tag{11}$$

$$\mathbf{B} = \beta^*\mathbf{C}_x + \alpha^*\mathbf{C}_x\mathbf{W}^H\mathbf{A}^H, \tag{12}$$

$$\mathbf{D} = |\beta|^2\mathbf{C}_x + \mathbf{C}_{ns} + |\alpha|^2\mathbf{A}\mathbf{W}\mathbf{C}_x\mathbf{W}^H\mathbf{A}^H + \alpha^*\beta\mathbf{C}_x\mathbf{W}^H\mathbf{A}^H + \alpha\beta^*\mathbf{A}\mathbf{W}\mathbf{C}_x. \tag{13}$$

One may resort to the maximum likelihood (ML) estimation, and the ML estimates can be obtained by

$$\min_{\boldsymbol{\theta} \triangleq [\beta, \alpha, \tau, f_d]^T} [\mathbf{y}^H\mathbf{C}_y^{-1}\mathbf{y} + \ln\det(\mathbf{C}_y)]. \tag{14}$$

Unfortunately, the ML cost function is highly non-linear. A brute force search over the multi-dimensional parameter space is computationally difficult. In the following, we consider alternative solutions by exploiting the expectation-maximization (EM) principle and approximations.

A. Em Estimator

The first step of the EM algorithm is to specify the "complete" data $\mathbf{z}$, whereas the observed data $\mathbf{y}$ is regarded as the "incomplete" data [22]. In our case, we can set $\mathbf{z}$ as

$$\mathbf{z} = [\mathbf{x}^T, \mathbf{y}^T]^T. \tag{15}$$

The EM algorithm starts with an initial guess of the parameters $\hat{\boldsymbol{\theta}}^{(0)}$. Given the parameter estimates obtained after the l-th iteration, $\hat{\boldsymbol{\theta}}^{(l)}$, the $(l+1)$-th iteration consists of an expectation step (E-step) followed by a maximization step (M-step):

E-step:

$$Q\left(\boldsymbol{\theta}; \hat{\boldsymbol{\theta}}^{(l)}\right) = E_{\mathbf{x}|\mathbf{y}, \hat{\boldsymbol{\theta}}^{(l)}}\{\log p(\mathbf{z}|\boldsymbol{\theta})\}. \tag{16}$$

[1] We assume τ is not discretized, i.e., it is arbitrary and not necessarily an integer multiple of T_s.

M-step:

$$\hat{\boldsymbol{\theta}}^{(l+1)} = \arg\max_{\boldsymbol{\theta}} Q\left(\boldsymbol{\theta}; \hat{\boldsymbol{\theta}}^{(l)}\right). \quad (17)$$

The E-step is precisely to find the expectation of the log-likelihood function (LLF) of the "complete" data $\mathbf{z}$, which is taken with respect to the signal waveform $\mathbf{x}$ and conditioned on observations $\mathbf{y}$ and $\hat{\boldsymbol{\theta}}^{(l)}$. The M-step is to maximize the expectation with respect to the unknown parameters. This iteration cycle is repeated until the algorithm converges, e.g., for some small tolerance ϵ,

$$\left\| \hat{\boldsymbol{\theta}}^{(l+1)} - \hat{\boldsymbol{\theta}}^{(l)} \right\| < \epsilon. \quad (18)$$

The expectation is computed in Appendix A. Furthermore, it is shown there that the maximization (17) is equivalent to

$$\hat{\boldsymbol{\theta}}^{(l+1)} = \arg\min_{\boldsymbol{\theta}} Q_1\left(\boldsymbol{\theta}; \hat{\boldsymbol{\theta}}^{(l)}\right), \quad (19)$$

where

$$Q_1\left(\boldsymbol{\theta}; \hat{\boldsymbol{\theta}}^{(l)}\right) = |\beta|^2 c_1^{(l)} + |\alpha|^2 c_2^{(l)}(\tau, f_d) + 2\Re\left\{\alpha\beta^* c_3^{(l)}(\tau, f_d) - \beta c_4^{(l)} - \alpha c_5^{(l)}(\tau, f_d)\right\} \quad (20)$$

with $c_1^{(l)}$, $c_2^{(l)}(\tau, f_d)$, $c_3^{(l)}(\tau, f_d)$, $c_4^{(l)}$, and $c_5^{(l)}(\tau, f_d)$ are defined in (56)–(60).

Jointly minimizing (20) with respect to the unknown parameters is still quite involved. Further simplifications can be made by using the person-by-person optimization idea [29]. Specifically, we partition the unknown parameters into three subsets as $\{\tau\}$, $\{f_d\}$, and $\{\alpha, \beta\}$, and minimize the cost function sequentially over these subsets. This leads to

$$\hat{\tau}^{(l+1)} = \arg\min_{\tau} Q_1\left(\tau, \hat{f}_d^{(l)}, \hat{\alpha}^{(l)}, \hat{\beta}^{(l)}; \hat{\boldsymbol{\theta}}^{(l)}\right), \quad (21)$$

$$\hat{f}_d^{(l+1)} = \arg\min_{f_d} Q_1\left(\hat{\tau}^{(l+1)}, f_d, \hat{\alpha}^{(l)}, \hat{\beta}^{(l)}; \hat{\boldsymbol{\theta}}^{(l)}\right), \quad (22)$$

$$\left\{\hat{\alpha}^{(l+1)}, \hat{\beta}^{(l+1)}\right\} = \arg\min_{\alpha,\beta} Q_1\left(\hat{\tau}^{(l+1)}, \hat{f}_d^{(l+1)}, \alpha, \beta; \hat{\boldsymbol{\theta}}^{(l)}\right). \quad (23)$$

The solutions to (21) and (22) can be obtained by using Newton's method, which is discussed in Appendix B. For the sub-problem (23), the cost function $Q_1(\hat{\tau}^{(l+1)}, \hat{f}_d^{(l+1)}, \alpha, \beta; \hat{\boldsymbol{\theta}}^{(l)})$ is a quadratic function with respect to α and β. Taking partial derivative of the cost function with respect to the conjugate of β and setting it equal to zero, we have

$$\bar{\beta}^{(l)}(\alpha) = \frac{1}{c_1^{(l)}}\left[\left(c_4^{(l)}\right)^* - \alpha c_3^{(l)}\right]. \quad (24)$$

Substituting (24) into the quadratic cost function, followed by taking the derivative with respect to the conjugate of α and setting to zero, we have

$$\hat{\alpha}^{(l+1)} = \frac{\left(\left(c_1^{(l)}\right)^* c_5^{(l)} - c_3^{(l)} c_4^{(l)}\right)^*}{c_1^{(l)} c_2^{(l)} - \left|c_3^{(l)}\right|^2}. \quad (25)$$

It follows that

$$\hat{\beta}^{(l+1)} = \bar{\beta}^{(l)}(\hat{\alpha}^{(l+1)}) = \frac{c_2^{(l)}\left(c_4^{(l)}\right)^* - c_3^{(l)}\left(c_5^{(l)}\right)^*}{c_1^{(l)} c_2^{(l)} - \left|c_3^{(l)}\right|^2}. \quad (26)$$

In the above equations, $c_2^{(l)}$, $c_3^{(l)}$, and $c_5^{(l)}$ are the resultant quantities obtained by substituting $\hat{\tau}^{(l+1)}$ and $\hat{f}_d^{(l+1)}$ into (57), (58), and (60), respectively.

Our proposed algorithm is summarized in Algorithm "EM Estimator".

Algorithm: EM Estimator

Input: observations $\mathbf{y}_r$ and $\mathbf{y}_s$, initial estimate of $\hat{\boldsymbol{\theta}}^{(0)}$, and convergence tolerance ϵ.

Output: an estimate of $\boldsymbol{\theta}$.

for $l = 0, 1, 2, \ldots$ **do**

1) Compute $\mathbf{B}^{(l)}$ and $\mathbf{D}^{(l)}$ by substituting the l-th estimate $\hat{\boldsymbol{\theta}}^{(l)}$ into (12) and (13).

2) Compute IO signal estimate $\hat{\mathbf{x}}^{(l)}$ and $\mathbf{C}_{xx|y}^{(l)}$ by (51) and (54).

3) Update the estimates of τ and f_d by solving (21) and (22).

4) Substitute the results in Step 2) and Step 3) into (56)–(60), and update the estimates of α and β using (25) and (26).

5) Check the stopping condition (18).

end for

return the latest estimate of $\boldsymbol{\theta}$.

Remark 1: Under the condition that the disturbance in the SC is white, we show in Appendix C that the M-step of the EM algorithm reduces to

$$\left\{\hat{\tau}^{(l+1)}, \hat{f}_d^{(l+1)}\right\} \approx \arg\max_{\tau, f_d} \Re\left\{\left(\mathbf{y}_s - \hat{\beta}^{(l)}\hat{\mathbf{x}}^{(l)}\right)^H \hat{\alpha}^{(l)}\mathbf{A}\mathbf{W}\hat{\mathbf{x}}^{(l)}\right\}. \quad (27)$$

It is noted that $(\mathbf{y}_s - \hat{\beta}^{(l)}\hat{\mathbf{x}}^{(l)})$ represents the observed SC signal after subtracting an estimated DPI based on the parameter estimates from the last iteration, and $\hat{\alpha}^{(l)}\mathbf{A}\mathbf{W}\hat{\mathbf{x}}^{(l)}$ represents an estimate of the target echo. Hence, the updating of τ and f_d estimates can be interpreted as DPI cancellation followed by a cross-correlation process.

Remark 2: To gain additional insight into the general scenario when the SC disturbance is colored, we show in Appendix C that the M-step of the EM algorithm can be written as

$$\left\{\hat{\tau}^{(l+1)}, \hat{f}_d^{(l+1)}\right\} \approx \arg\min_{\tau, f_d} \left\|\mathbf{C}_{ns}^{-\frac{1}{2}}\left(\mathbf{y}_s - \hat{\beta}^{(l)}\hat{\mathbf{x}}^{(l)} - \hat{\alpha}^{(l)}\mathbf{A}\mathbf{W}\hat{\mathbf{x}}^{(l)}\right)\right\|^2. \quad (28)$$

It is seen that updating τ and f_d is equivalent to solving a *weighted least squares* problem. The weighting matrix is the disturbance covariance matrix in the SC.

B. Modified Cross-Correlation Estimator

Based on the above remarks, we introduce a modified CC (MCC) estimator by taking into account the effect of DPI. The MCC first obtains a coarse estimate of the DPI amplitude as

$$\bar{\beta} = \frac{\mathbf{y}_r^H \mathbf{y}_s}{\|\mathbf{y}_r\|^2}. \tag{29}$$

Then, τ and f_d can be estimated by

$$\left\{\hat{\tau}, \hat{f}_d\right\} = \arg\max_{\tau, f_d} \left|(\mathbf{y}_s - \bar{\beta}\mathbf{y}_r)^H \mathbf{A}(f_d)\mathbf{W}(\tau)\mathbf{y}_r\right|. \tag{30}$$

Finally, the amplitudes can be estimated as

$$\hat{\alpha} = \frac{d_2 d_4 - d_1 d_3^*}{d_2^2 - |d_3|^2}, \tag{31}$$

$$\hat{\beta} = \frac{d_1 d_2 - d_3 d_4}{d_2^2 - |d_3|^2}, \tag{32}$$

where $d_1 = \mathbf{y}_r^H \mathbf{y}_s$, $d_2 = \|\mathbf{y}_r\|^2$, $d_3 = \mathbf{y}_r^H \mathbf{A}(\hat{f}_d)\mathbf{W}(\hat{\tau})\mathbf{y}_r$, and $d_4 = (\mathbf{A}(\hat{f}_d)\mathbf{W}(\hat{\tau})\mathbf{y}_r)^H \mathbf{y}_s$. The MCC estimator is computationally more efficient than the EM estimator. Clearly, the MCC method reduces to the conventional CC method by ignoring the DPI, i.e., by setting $\bar{\beta} = 0$.

C. CRLB

To benchmark the proposed estimators, the CRLB for the considered estimation problem is calculated next. Since the amplitude parameters β and α are complex, we define the real parameter vector $\boldsymbol{\xi} = [\xi_1, \xi_2, \ldots, \xi_6]^T = [\beta_R, \beta_I, \alpha_R, \alpha_I, \tau, f_d]^T$ where $\beta = \beta_R + j\beta_I$ and $\alpha = \alpha_R + j\alpha_I$. Using the *Slepian-Bangs* formula [30, p. 525], the entries of the 6-by-6 Fisher information matrix (FIM) $\mathbf{F}$ are

$$[\mathbf{F}]_{p,q} = \mathrm{tr}\left\{\mathbf{C}_y^{-1}\frac{\partial \mathbf{C}_y}{\partial \xi_p}\mathbf{C}_y^{-1}\frac{\partial \mathbf{C}_y}{\partial \xi_q}\right\} \text{ for } p, q = 1, 2, \ldots, 6, \tag{33}$$

where

$$\frac{\partial \mathbf{C}_y}{\partial \xi_p} = \begin{bmatrix} \mathbf{0}_{M\times M} & \mathbf{B}_p \\ \mathbf{B}_p^H & \mathbf{D}_p \end{bmatrix} \text{ for } p = 1, 2, \ldots, 6, \tag{34}$$

and

$$\begin{aligned}
\mathbf{B}_1 &= \mathbf{C}_x,\ \mathbf{B}_2 = -j\mathbf{B}_1,\\
\mathbf{B}_3 &= \mathbf{C}_x\mathbf{W}^H\mathbf{A}^H,\ \mathbf{B}_4 = -j\mathbf{B}_3,\\
\mathbf{B}_5 &= \alpha^*\mathbf{C}_x\dot{\mathbf{W}}^H\mathbf{A}^H,\\
\mathbf{B}_6 &= \alpha^*\mathbf{C}_x\mathbf{W}^H\dot{\mathbf{A}}^H,\\
\mathbf{D}_1 &= 2\beta_R\mathbf{C}_x + \alpha^*\mathbf{B}_3 + \alpha\mathbf{B}_3^H,\\
\mathbf{D}_2 &= 2\beta_I\mathbf{C}_x - \alpha^*\mathbf{B}_4 - \alpha\mathbf{B}_4^H,\\
\mathbf{D}_3 &= 2\alpha_R\mathbf{A}\mathbf{W}\mathbf{C}_x\mathbf{W}^H\mathbf{A}^H + \beta\mathbf{B}_3 + \beta^*\mathbf{B}_3^H,\\
\mathbf{D}_4 &= 2\alpha_I\mathbf{A}\mathbf{W}\mathbf{C}_x\mathbf{W}^H\mathbf{A}^H + \beta\mathbf{B}_4 + \beta^*\mathbf{B}_4^H,\\
\mathbf{D}_5 &= |\alpha|^2(\mathbf{A}\dot{\mathbf{W}}\mathbf{C}_x\mathbf{W}^H\mathbf{A}^H + \mathbf{A}\mathbf{W}\mathbf{C}_x\dot{\mathbf{W}}^H\mathbf{A}^H)\\
&\quad + \beta\mathbf{B}_5 + \beta^*\mathbf{B}_5^H,\\
\mathbf{D}_6 &= |\alpha|^2(\dot{\mathbf{A}}\mathbf{W}\mathbf{C}_x\mathbf{W}^H\mathbf{A}^H + \mathbf{A}\mathbf{W}\mathbf{C}_x\mathbf{W}^H\dot{\mathbf{A}}^H)\\
&\quad + \beta\mathbf{B}_6 + \beta^*\mathbf{B}_6^H.
\end{aligned}$$

The matrices $\dot{\mathbf{W}}$ and $\dot{\mathbf{A}}$ are given by (68) and (73), respectively, in Appendix B. Consequently,

$$\mathrm{CRLB}_{\xi_p} = [\mathbf{F}^{-1}]_{p,p} \text{ for } p = 1, 2, \ldots, 6. \tag{35}$$

TABLE I
PARAMETERS USED IN SIMULATIONS

M	f_s	$\lfloor T \rfloor$	τ	f_d	a_1	$\lvert\lambda\rvert^2$	$\lvert\alpha\rvert^2$
256	1	199	24.78	$\frac{25.11}{M}$	-0.9	1	1

IV. Numerical Simulations

In our simulations, we use a first-order autoregressive AR (1) process to model the narrowband IO signal $\{x(m)\}$. The AR coefficient and noise variance of the AR (1) process are denoted by a_1 and σ^2, respectively. Let $\sigma^2 = 1 - |a_1|^2$, so that the AR (1) process has unit average power with an auto-correlation function given by $r(k) = (-a_1)^k, k \geq 0$. The temporal covariance matrix $\mathbf{R}_x$ of the IO waveform is

$$\mathbf{R}_x = |\lambda|^2 \begin{bmatrix} \mathbf{R}_t & \mathbf{0} \\ \mathbf{0} & \mathbf{0} \end{bmatrix}, \tag{36}$$

where $[\mathbf{R}_t]_{p,q} = r(p-q)$ for $p, q = 1, 2, \ldots, \lfloor \frac{T}{T_s} + 1 \rfloor$ and $|\lambda|^2$ is the average power of the IO waveform. We assume that the disturbance in the RC and SC is zero-mean white Gaussian distributed with covariance matrices: $\mathbf{C}_{nr} = \mathbf{R}_{nr} = \sigma_{nr}^2\mathbf{I}_M, \mathbf{C}_{ns} = \mathbf{R}_{ns} = \sigma_{ns}^2\mathbf{I}_M$. The signal-to-noise ratio (SNR) in the RC is defined as

$$\mathrm{SNR}_r = \frac{|\lambda|^2 \cdot \lfloor \frac{T}{T_s} + 1 \rfloor}{M\sigma_{nr}^2}, \tag{37}$$

the DPI-to-noise ratio (DNR) in the SC is

$$\mathrm{DNR}_s = \frac{|\lambda|^2|\beta|^2 \cdot \lfloor \frac{T}{T_s} + 1 \rfloor}{M\sigma_{ns}^2}, \tag{38}$$

and the SNR in the SC is

$$\mathrm{SNR}_s = \frac{|\lambda|^2|\alpha|^2 \cdot \lfloor \frac{T}{T_s} + 1 \rfloor}{M\sigma_{ns}^2}. \tag{39}$$

Assuming that the IO employs a framed transmission with a frame length of T seconds, $\lfloor \frac{T}{T_s} + 1 \rfloor$ in the above expressions denotes the number of IO signal samples. As explained in Section II, the observation window has $M \geq \lfloor \frac{T}{T_s} + 1 \rfloor$ samples to include possible bistatic delay of the target. So, out of the M observed samples used for estimation, there are only $\lfloor \frac{T}{T_s} + 1 \rfloor$ non-zero signal samples, which is why the normalization factor of $\lfloor \frac{T}{T_s} + 1 \rfloor / M$ is included in the above definitions. The parameters used in simulations are shown in Table I. Note that the sampling rate is normalized as $f_s = 1$, and thus $T_s = 1$.

For delay and Doppler frequency estimation, we use Monte Carlo simulations to measure the mean-square errors (MSEs) of the considered estimators according to $\mathrm{MSE}_\tau = E\{|\hat{\tau} - \tau|^2\}$ and $\mathrm{MSE}_f = M^2 E\{|\hat{f}_d - f_d|^2\}$, respectively. Note that the Doppler frequency estimate is normalized by $1/M$, which represents the *bin spacing* in Doppler processing. Hence, the MSE_f can be interpreted as the estimation accuracy relative to the Fourier resolution. For amplitude estimation, we use the normalized standard deviation (NSD) defined as $\mathrm{NSD}_\alpha = (\sqrt{E\{|\hat{\alpha} - \alpha|^2\}} / |\alpha|) \times 100\%$. The reason for using the NSD is because the parameter may change with different SNR (as in Fig. 2), and the normalization helps to see the trend as the SNR changes. The definition for NSD_β is similar.

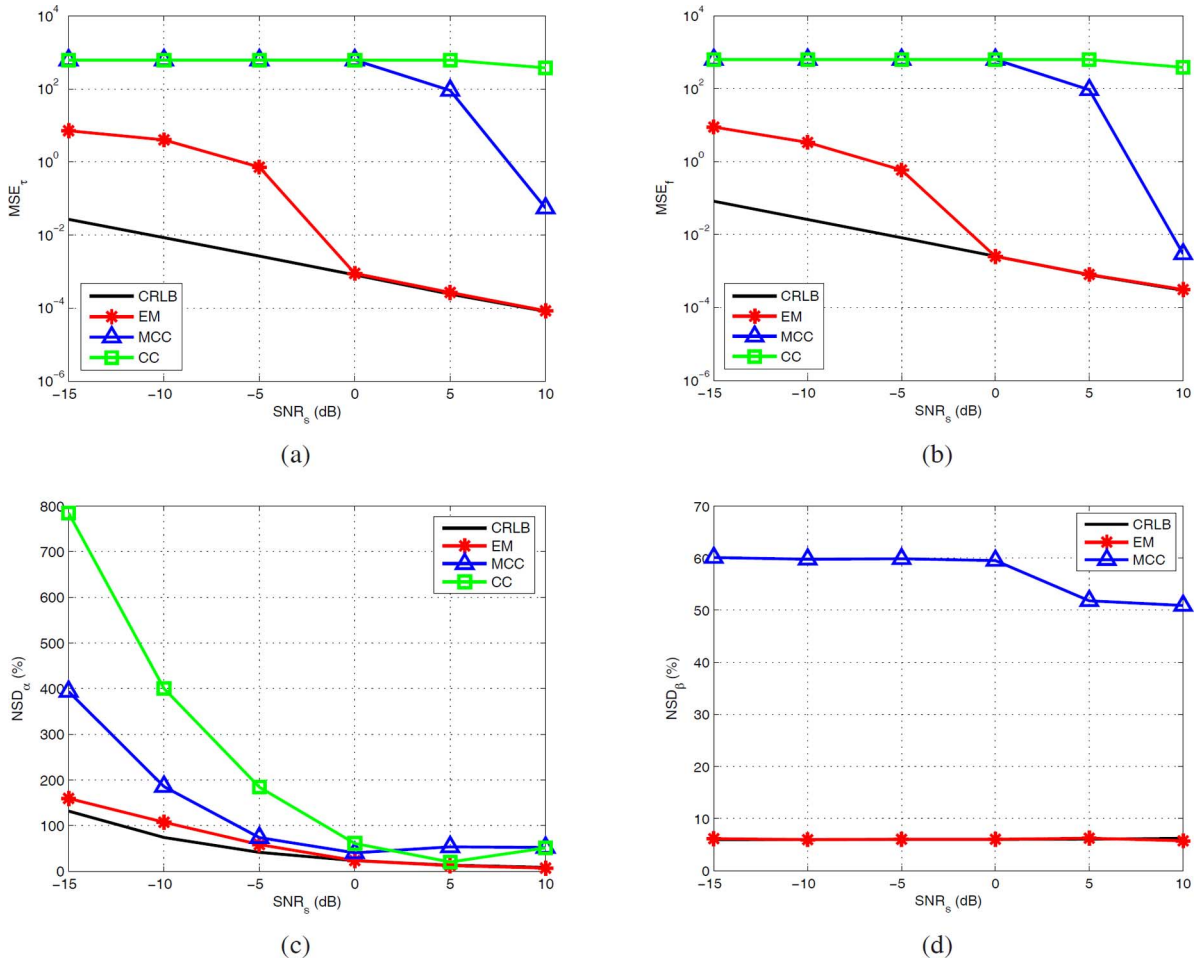

Fig. 2. Performance comparisons with $\mathrm{SNR}_r = 0$ dB and $\mathrm{DNR}_s = 10$ dB. (a) time delay; (b) Doppler frequency; (c) target echo amplitude; (d) DPI amplitude.

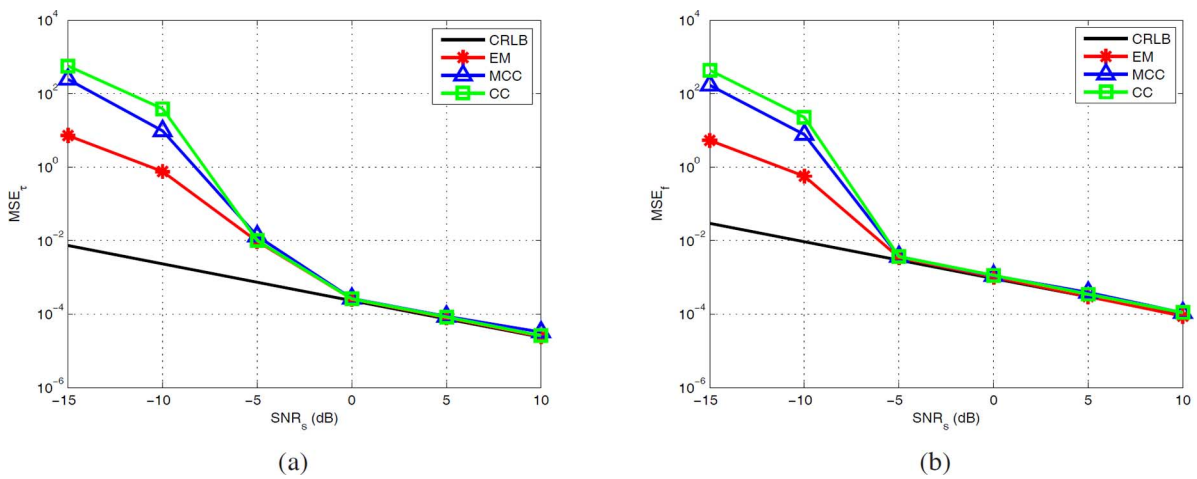

Fig. 3. Performance comparisons with $\mathrm{SNR}_r = 30$ dB and $\mathrm{DNR}_s = -20$ dB. (a) time delay; (b) Doppler frequency.

Fig. 2 considers a scenario where the *RC is noisy* ($\mathrm{SNR}_r = 0$ dB) and the *DPI in the SC is strong* ($\mathrm{DNR}_s = 10$ dB). Note that the conventional CC estimator cannot provide the estimate of β and hence is not included in Fig. 2(d). It is seen that the EM estimator is the best in this scenario and achieves the CRLB as SNR_s increases. In addition, the MCC estimator is worse than the EM estimator, but outperforms the CC estimator. The CC estimator fails completely in this scenario, mainly because of the strong DPI in the SC. The MCC estimator, also affected by the DPI, is able to correctly locate the target only when SNR_s is high enough.

In contrast to Fig. 2, Fig. 3 considers a more *benign environment* with $\mathrm{DNR}_s = -20$ dB and $\mathrm{SNR}_r = 30$ dB. In this case, the EM estimator still outperforms the MCC and CC estimators

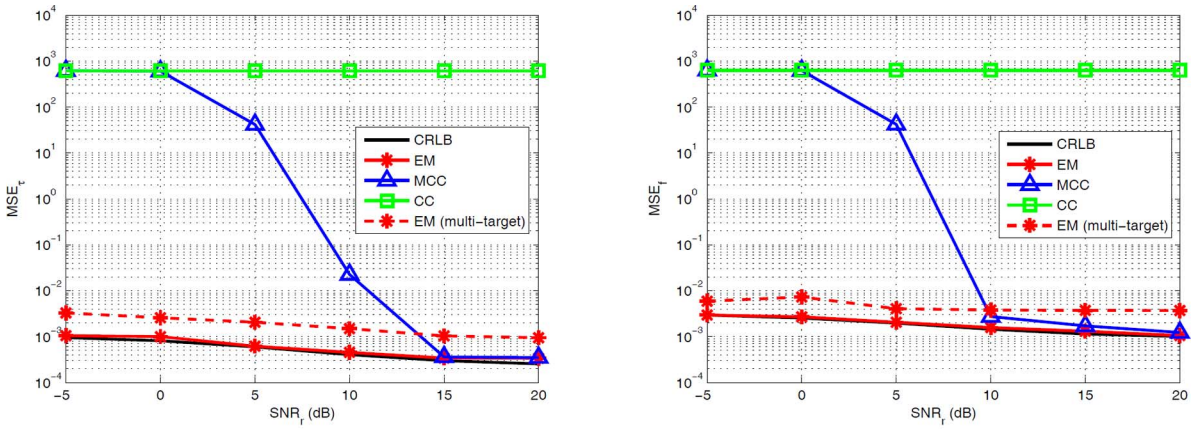

Fig. 4. Performance comparisons with $\mathrm{DNR}_s = 10$ dB and $\mathrm{SNR}_s = 0$ dB. (a) time delay; (b) Doppler frequency.

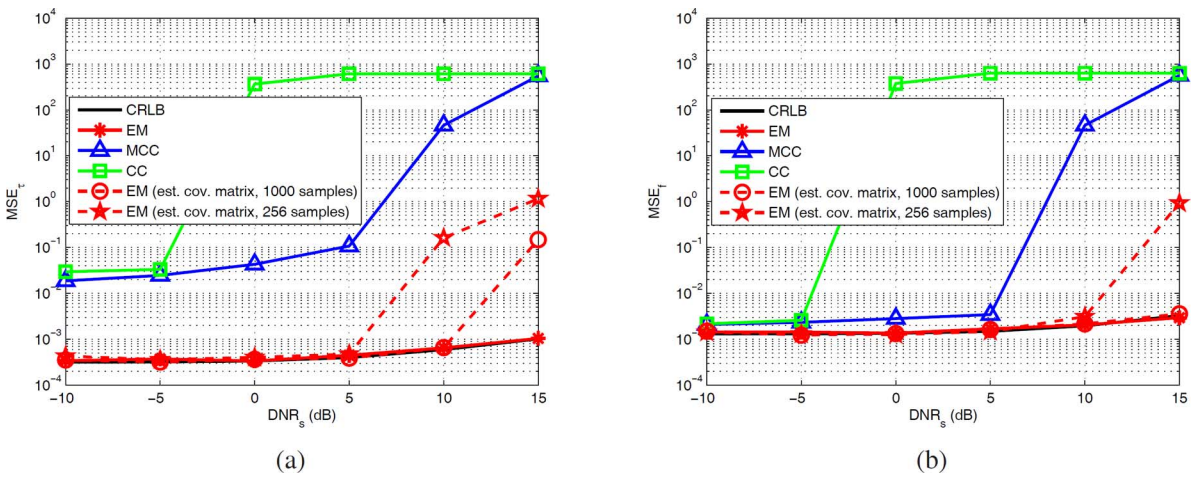

Fig. 5. Performance comparisons with $\mathrm{SNR}_r = 5$ dB and $\mathrm{SNR}_s = 0$ dB. (a) time delay; (b) Doppler frequency.

in the low SNR_s region. As SNR_s increases, the performances of all three estimators are similar and approach the CRLB. As expected, the CC estimator performs very close to the MCC estimator in this case, due to the fact that the DPI in the SC is very weak. A comparison of Figs. 2 and 3 reveals that the MCC and CC estimators are sensitive to the quality of the reference signal as well as the DPI, while the EM estimator is more robust against these factors.

Fig. 4 depicts the estimation performance with respect to SNR_r when $\mathrm{DNR}_s = 10$ dB and $\mathrm{SNR}_s = 0$ dB . This parameter setting indicates that the target echo is much weaker than the DPI and can be easily masked by the DPI or its sidelobes. Again, we observe that the CC estimator does not work at all, even when the reference signal in the RC becomes very clean. This result is still due to the fact that the CC cannot handle a strong DPI. The EM estimator outperforms the MCC and CC estimators, especially at low SNR_r, where the EM curve is also very close to the CRLB. It can be seen that the MCC estimator improves with the SNR_r and approaches the EM performance. Besides, when the RC is noisy (i.e., in the low SNR_r region), the performance of the MCC estimator can not be differentiated from that of the CC estimator because of the ineffective DPI cancellation (also seen in Fig. 2).

In this simulation, we also consider the effect of multiple targets to the proposed EM estimator. We simulated a two-target scenario, where the first target has the same parameters as before, while the second target has a delay of 20 and a Doppler frequency of $21/M$, and an SNR of -5 dB . The delay and Doppler estimation performance of the EM estimator for the first target is included in Fig. 4 as "EM (multi-target)". It is seen that there is some degradation of the EM estimator in the presence of multiple targets relative to the single-target case, but the estimator is still functional. The reason can be seen from Remark 1 in Section III-A. In essence, following DPI cancellation, the EM estimator uses a peak finding procedure to obtain the delay and Doppler estimates. With multiple targets, the procedure is able to identify the strongest target. The weaker targets can be estimated by subtracting the stronger ones and a similar peak finding procedure. It should be noted that at sufficiently high SNR_r, EM (multi-target) becomes slightly worse than MCC, which is expected, since for the latter, the signal contains only a single target.

Fig. 5 provides the performance comparison with respect to DNR_s, where SNR_r and SNR_s are fixed at 5 dB and 0 dB, respectively. From this figure, we see that the EM estimator still has the best performance and can achieve the CRLB. In par-

ticular, it is seen that the EM estimator is robust to the DPI. Both the MCC and CC estimators are sensitive to DPI and the MCC estimator outperforms the CC estimator when the DPI is moderate. The EM estimator requires the signal covariance matrix $\mathbf{C}_x$, which may be unknown and needs to be estimated. In Fig. 5, we have also included the performance of the EM estimator with an estimated covariance matrix $\hat{\mathbf{C}}_x$, which is obtained by using the reference signal. Specifically, we use the unbiased correlation estimator on the reference signal to estimate the signal correlation sequence, which is windowed by using a tapering window, and a Toeplitz covariance matrix estimate $\hat{\mathbf{C}}_x$ is formed by the windowed correlation sequence. The results are shown in Fig. 5 as "EM (est. cov. matrix, 256 samples)" and "EM (est. cov. matrix, 1000 samples)". Two cases are included. The first uses only the $M = 256$ samples from the reference channel to estimate $\hat{\mathbf{C}}_x$; these are the same reference signal samples used by all other estimators and, hence, no extra training data is involved. In the second case, $\hat{\mathbf{C}}_x$ is estimated with 1000 samples from the training data. It is seen from Fig. 5 that, as expected, there is some degradation of the EM estimator, and the degradation decreases as more training data is available.

Finally, we consider the computational complexity of the CC, MCC, and EM methods. As pointed out earlier, the EM estimator is notably more involved than the other methods. To provide more details, we numerically measure the complexity by the *elapsed time* in Matlab, using a PC running Matlab R2013b in Windows 7 Professional (64-bit) with 3.30 GHz CPU and 8 GB RAM. For the set-up in Fig. 5, the CC estimator needs 0.37 seconds on average, the MCC estimator needs 0.42 seconds, while the EM estimator needs 5.83 seconds. Hence, the proposed EM estimator achieves the improved estimation accuracy at the cost of higher complexity.

V. Conclusion

In this paper, we examined the joint delay and Doppler estimation problem for passive sensing in the presence of disturbance (clutter and noise) and DPI. Unlike conventional methods, our approach treats the delay and Doppler as continuous parameters without discretization. We proposed an EM based estimator as well as an MCC estimator which is computationally more efficient. We also derived the CRLB for the joint estimation problem. Numerical results show that the EM estimator significantly outperforms the MCC and CC estimators when the RC is noisy and the DPI is stronger than the target echo. Under this challenging condition, the MCC estimator enjoys some benefits provided by DPI cancellation and is notably better than the CC. When the RC is clean and the DPI is weaker than the target echo, the EM estimator still outperforms the other approaches in the low SNR_s region, but that advantage diminishes as SNR_s increases. In general, the MCC and CC estimators are more sensitive to the quality of the reference signal and the DPI effects than the EM estimator. The CRLB is provided as a benchmark of the estimation performance. It is shown that the performance of the EM estimator is very close to the predicted accuracy.

Appendix A
Proof of (19)

The likelihood function of the "complete" data $\mathbf{z} = [\mathbf{x}^T, \mathbf{y}^T]^T$ is

$$p(\mathbf{z}|\boldsymbol{\theta}) = p(\mathbf{y}|\mathbf{x},\boldsymbol{\theta})p(\mathbf{x}|\boldsymbol{\theta}) = \frac{1}{\det(\pi\mathbf{C}_x)\det(\pi\mathbf{C}_{2M})} \times \exp\Big\{ -\mathbf{x}^H\mathbf{C}_x^{-1}\mathbf{x} - (\mathbf{y}_r-\mathbf{x})^H\mathbf{C}_{nr}^{-1}(\mathbf{y}_r-\mathbf{x}) - (\mathbf{y}_s-\beta\mathbf{x}-\alpha\mathbf{A}\mathbf{W}\mathbf{x})^H\mathbf{C}_{ns}^{-1}(\mathbf{y}_s-\beta\mathbf{x}-\alpha\mathbf{A}\mathbf{W}\mathbf{x})\Big\}, \quad (40)$$

where

$$\mathbf{C}_{2M} = \begin{bmatrix} \mathbf{C}_{nr} & \mathbf{0}_{M\times M} \\ \mathbf{0}_{M\times M} & \mathbf{C}_{ns} \end{bmatrix}. \quad (41)$$

Thus, the LLF can be written as

$$\log p(\mathbf{z}|\boldsymbol{\theta}) = s_1(\mathbf{x}) - s_2(\mathbf{x},\boldsymbol{\theta}), \quad (42)$$

where

$$s_1(\mathbf{x}) = -\ln\det(\pi\mathbf{C}_x) - \ln\det(\pi\mathbf{C}_{2M}) - \mathbf{x}^H\mathbf{C}_x^{-1}\mathbf{x} - (\mathbf{y}_r-\mathbf{x})^H\mathbf{C}_{nr}^{-1}(\mathbf{y}_r-\mathbf{x}) - \mathbf{y}_s^H\mathbf{C}_{ns}^{-1}\mathbf{y}_s, \quad (43)$$

$$s_2(\mathbf{x},\boldsymbol{\theta}) = |\beta|^2\mathbf{x}^H\mathbf{C}_{ns}^{-1}\mathbf{x} + |\alpha|^2\mathbf{x}^H\mathbf{W}^H\mathbf{A}^H\mathbf{C}_{ns}^{-1}\mathbf{A}\mathbf{W}\mathbf{x} + 2\Re\Big\{\alpha\beta^*\mathbf{x}^H\mathbf{C}_{ns}^{-1}\mathbf{A}\mathbf{W}\mathbf{x} - \beta\mathbf{y}_s^H\mathbf{C}_{ns}^{-1}\mathbf{x} - \alpha\mathbf{y}_s^H\mathbf{C}_{ns}^{-1}\mathbf{A}\mathbf{W}\mathbf{x}\Big\}. \quad (44)$$

The cost function is consequently given by

$$Q\left(\boldsymbol{\theta};\hat{\boldsymbol{\theta}}^{(l)}\right) = E_{\mathbf{x}|\mathbf{y},\hat{\boldsymbol{\theta}}^{(l)}}\left\{s_1(\mathbf{x})\right\} - E_{\mathbf{x}|\mathbf{y},\hat{\boldsymbol{\theta}}^{(l)}}\left\{s_2(\mathbf{x},\boldsymbol{\theta})\right\}. \quad (45)$$

Note that only the second term in (45) involves the parameters to be estimated and that the first term is constant in the M-step. Therefore, we have the following result for the M-step,

$$\arg\max_{\boldsymbol{\theta}} Q\left(\boldsymbol{\theta};\hat{\boldsymbol{\theta}}^{(l)}\right) = \arg\min_{\boldsymbol{\theta}} Q_1\left(\boldsymbol{\theta};\hat{\boldsymbol{\theta}}^{(l)}\right), \quad (46)$$

where

$$Q_1\left(\boldsymbol{\theta};\hat{\boldsymbol{\theta}}^{(l)}\right) = E_{\mathbf{x}|\mathbf{y},\hat{\boldsymbol{\theta}}^{(l)}}\left\{s_2(\mathbf{x},\boldsymbol{\theta})\right\}. \quad (47)$$

Next, we find an explicit expression for $Q_1\left(\boldsymbol{\theta};\hat{\boldsymbol{\theta}}^{(l)}\right)$. Let

$$\hat{\mathbf{x}}^{(l)} = E_{\mathbf{x}|\mathbf{y},\hat{\boldsymbol{\theta}}^{(l)}}\{\mathbf{x}\}. \quad (48)$$

Since $\mathbf{x}$ and $\mathbf{y}$ are jointly Gaussian, $\hat{\mathbf{x}}^{(l)}$ has a closed-form expression. By denoting

$$\mathbf{C}_{xy}^{(l)} = E_{\mathbf{x}|\hat{\boldsymbol{\theta}}^{(l)}}\left\{\mathbf{x}\mathbf{y}^H\right\} = [\,\mathbf{C}_x \quad \mathbf{B}^{(l)}\,], \quad (49)$$

$$\mathbf{C}_{yy}^{(l)} = E_{\mathbf{x}|\hat{\boldsymbol{\theta}}^{(l)}}\{\mathbf{y}\mathbf{y}^H\} = \begin{bmatrix} \mathbf{G} & \mathbf{B}^{(l)} \\ (\mathbf{B}^{(l)})^H & \mathbf{D}^{(l)} \end{bmatrix}, \quad (50)$$

where $\mathbf{B}^{(l)}$ and $\mathbf{D}^{(l)}$ are obtained by substituting the l-th estimate $\hat{\boldsymbol{\theta}}^{(l)}$ into (12) and (13), respectively, we have [30, p. 324]

$$\begin{aligned}\hat{\mathbf{x}}^{(l)} &= E\{\mathbf{x}\} + \mathbf{C}_{xy}^{(l)}\left(\mathbf{C}_{yy}^{(l)}\right)^{-1}(\mathbf{y} - E\{\mathbf{y}\}) \\ &= \mathbf{C}_{xy}^{(l)}\left(\mathbf{C}_{yy}^{(l)}\right)^{-1}\mathbf{y} \\ &= \mathbf{C}_{nr}\mathbf{G}^{-1}\mathbf{B}^{(l)}\mathbf{S}_G^{-1}\mathbf{y}_s + \mathbf{y}_r - \mathbf{C}_{nr}\mathbf{S}_D^{-1}\mathbf{y}_r, \quad (51)\end{aligned}$$

where the third equality is obtained by using the block matrix inversion formula [31], and the *Schur complements* $\mathbf{S}_G$ and $\mathbf{S}_D$ are defined by

$$\mathbf{S}_G = \mathbf{D}^{(l)} - \left(\mathbf{B}^{(l)}\right)^H \mathbf{G}^{-1}\mathbf{B}^{(l)}, \quad (52)$$

$$\mathbf{S}_D = \mathbf{G} - \mathbf{B}^{(l)}\left(\mathbf{D}^{(l)}\right)^{-1}\left(\mathbf{B}^{(l)}\right)^H. \quad (53)$$

Consequently,

$$\begin{aligned}\mathbf{C}_{xx|y}^{(l)} &= E_{\mathbf{x}|\mathbf{y},\hat{\boldsymbol{\theta}}^{(l)}}\{\mathbf{x}\mathbf{x}^H\} \\ &= \hat{\mathbf{x}}^{(l)}\left(\hat{\mathbf{x}}^{(l)}\right)^H + E_{\mathbf{x}|\mathbf{y},\hat{\boldsymbol{\theta}}^{(l)}}\left\{\left(\mathbf{x} - \hat{\mathbf{x}}^{(l)}\right)\left(\mathbf{x} - \hat{\mathbf{x}}^{(l)}\right)^H\right\} \\ &= \hat{\mathbf{x}}^{(l)}\left(\hat{\mathbf{x}}^{(l)}\right)^H + \mathbf{C}_x - \mathbf{C}_{xy}^{(l)}\left(\mathbf{C}_{yy}^{(l)}\right)^{-1}\left(\mathbf{C}_{xy}^{(l)}\right)^H \\ &= \hat{\mathbf{x}}^{(l)}\left(\hat{\mathbf{x}}^{(l)}\right)^H + \mathbf{C}_{nr} - \mathbf{C}_{nr}\mathbf{S}_D^{-1}\mathbf{C}_{nr}, \quad (54)\end{aligned}$$

where the fourth equality is also a result of using the block matrix inversion formula. Finally, we get

$$\begin{aligned}Q_1\left(\boldsymbol{\theta};\hat{\boldsymbol{\theta}}^{(l)}\right) &= |\beta|^2 c_1^{(l)} + |\alpha|^2 c_2^{(l)}(\tau, f_d) \\ &\quad + 2\Re\left\{\alpha\beta^* c_3^{(l)}(\tau, f_d) - \beta c_4^{(l)} - \alpha c_5^{(l)}(\tau, f_d)\right\}, \quad (55)\end{aligned}$$

where

$$\begin{aligned}c_1^{(l)} &= E_{\mathbf{x}|\mathbf{y},\hat{\boldsymbol{\theta}}^{(l)}}\{\mathbf{x}^H\mathbf{C}_{ns}^{-1}\mathbf{x}\} \\ &= \mathrm{tr}\left\{\mathbf{C}_{ns}^{-1}\mathbf{C}_{xx|y}^{(l)}\right\}, \quad (56) \\ c_2^{(l)}(\tau, f_d) &= E_{\mathbf{x}|\mathbf{y},\hat{\boldsymbol{\theta}}^{(l)}}\{\mathbf{x}^H\mathbf{W}^H\mathbf{A}^H\mathbf{C}_{ns}^{-1}\mathbf{A}\mathbf{W}\mathbf{x}\} \\ &= \mathrm{tr}\left\{\mathbf{W}\mathbf{C}_{xx|y}^{(l)}\mathbf{W}^H\mathbf{A}^H\mathbf{C}_{ns}^{-1}\mathbf{A}\right\}, \quad (57) \\ c_3^{(l)}(\tau, f_d) &= E_{\mathbf{x}|\mathbf{y},\hat{\boldsymbol{\theta}}^{(l)}}\left\{\mathbf{x}^H\mathbf{C}_{ns}^{-1}\mathbf{A}\mathbf{W}\mathbf{x}\right\} \\ &= \mathrm{tr}\left\{\mathbf{C}_{ns}^{-1}\mathbf{A}\mathbf{W}\mathbf{C}_{xx|y}^{(l)}\right\}, \quad (58) \\ c_4^{(l)} &= E_{\mathbf{x}|\mathbf{y},\hat{\boldsymbol{\theta}}^{(l)}}\left\{\mathbf{y}_s^H\mathbf{C}_{ns}^{-1}\mathbf{x}\right\} \\ &= \mathbf{y}_s^H\mathbf{C}_{ns}^{-1}\hat{\mathbf{x}}^{(l)}, \quad (59) \\ c_5^{(l)}(\tau, f_d) &= E_{\mathbf{x}|\mathbf{y},\hat{\boldsymbol{\theta}}^{(l)}}\{\mathbf{y}_s^H\mathbf{C}_{ns}^{-1}\mathbf{A}\mathbf{W}\mathbf{x}\} \\ &= \mathbf{y}_s^H\mathbf{C}_{ns}^{-1}\mathbf{A}\mathbf{W}\hat{\mathbf{x}}^{(l)}. \quad (60)\end{aligned}$$

Appendix B
Solution to (21) and (22)

To solve (21), a coarse one-dimensional search is conducted to find an initial estimate. Then, the solution is refined by exploiting the following necessary condition of optimality

$$g\left(\hat{\tau}^{(l+1)}\right) = 0, \quad (61)$$

where

$$g(\tau) = \frac{\partial Q_1\left(\tau, \hat{f}_d^{(l)}, \hat{\alpha}^{(l)}, \hat{\beta}^{(l)}; \hat{\boldsymbol{\theta}}^{(l)}\right)}{\partial\tau}. \quad (62)$$

Newton's method is used to find the root of the first derivative $g(\tau)$ in the neighborhood of the initial estimate. Specifically, at the m-th iteration of Newton's method, we compute

$$\tau_m = \tau_{m-1} - \frac{g(\tau_{m-1})}{g'(\tau_{m-1})}, \quad (63)$$

where $g'(\tau)$ is the gradient

$$g'(\tau) = \frac{\partial^2 Q_1\left(\tau, \hat{f}_d^{(l)}, \hat{\alpha}^{(l)}, \hat{\beta}^{(l)}; \hat{\boldsymbol{\theta}}^{(l)}\right)}{\partial\tau^2}. \quad (64)$$

This process is repeated until convergence.

The first two derivatives $g(\tau)$ and $g'(\tau)$ are obtained using the following results:

$$\begin{aligned}&\frac{\partial Q_1\left(\boldsymbol{\theta};\hat{\boldsymbol{\theta}}^{(l)}\right)}{\partial\tau} \\ &= |\alpha|^2\mathrm{tr}\left\{\left(\dot{\mathbf{W}}\mathbf{C}_{xx|y}^{(l)}\mathbf{W}^H + \mathbf{W}\mathbf{C}_{xx|y}^{(l)}\dot{\mathbf{W}}^H\right)\mathbf{A}^H\mathbf{C}_{ns}^{-1}\mathbf{A}\right\} \\ &\quad + 2\Re\left\{\mathrm{tr}\left\{\alpha\mathbf{C}_{ns}^{-1}\mathbf{A}\dot{\mathbf{W}}\left(\beta^*\mathbf{C}_{xx|y}^{(l)} - \hat{\mathbf{x}}^{(l)}\mathbf{y}_s^H\right)\right\}\right\}, \quad (65)\end{aligned}$$

and

$$\begin{aligned}&\frac{\partial^2 Q_1\left(\boldsymbol{\theta};\hat{\boldsymbol{\theta}}^{(l)}\right)}{\partial\tau^2} = |\alpha|^2\mathrm{tr}\Big\{\left(\ddot{\mathbf{W}}\mathbf{C}_{xx|y}^{(l)}\mathbf{W}^H + 2\dot{\mathbf{W}}\mathbf{C}_{xx|y}^{(l)}\dot{\mathbf{W}}^H\right. \\ &\left.+ \mathbf{W}\mathbf{C}_{xx|y}^{(l)}\ddot{\mathbf{W}}^H\right)\mathbf{A}^H\mathbf{C}_{ns}^{-1}\mathbf{A}\Big\} + 2\Re\Big\{\mathrm{tr}\Big\{\alpha\mathbf{C}_{ns}^{-1}\mathbf{A}\ddot{\mathbf{W}} \\ &\times\left(\beta^*\mathbf{C}_{xx|y}^{(l)} - \hat{\mathbf{x}}^{(l)}\mathbf{y}_s^H\right)\Big\}\Big\}, \quad (66)\end{aligned}$$

where

$$\dot{\mathbf{W}} = \frac{\partial\mathbf{W}}{\partial\tau} \text{ and } \ddot{\mathbf{W}} = \frac{\partial^2\mathbf{W}}{\partial\tau^2}. \quad (67)$$

The diagonal matrices $\dot{\mathbf{W}}$ and $\ddot{\mathbf{W}}$ have diagonal entries

$$[\dot{\mathbf{W}}]_{p,p} = -j2\pi\Delta f(p-1)e^{-j2\pi\Delta f(p-1)\tau}, \quad (68)$$

and

$$[\ddot{\mathbf{W}}]_{p,p} = -4[\pi\Delta f(p-1)]^2 e^{-j2\pi\Delta f(p-1)\tau}, \quad (69)$$

respectively, for $p = 1, 2, \ldots, M$.

A similar Newton's approach can be applied to (22), where

$$\begin{aligned}&\frac{\partial Q_1\left(\boldsymbol{\theta};\hat{\boldsymbol{\theta}}^{(l)}\right)}{\partial f_d} \\ &= |\alpha|^2\mathrm{tr}\left\{\mathbf{W}\mathbf{C}_{xx|y}^{(l)}\mathbf{W}^H\left(\dot{\mathbf{A}}^H\mathbf{C}_{ns}^{-1}\mathbf{A} + \mathbf{A}^H\mathbf{C}_{ns}^{-1}\dot{\mathbf{A}}\right)\right\} \\ &\quad + 2\Re\left\{\mathrm{tr}\left\{\alpha\mathbf{C}_{ns}^{-1}\dot{\mathbf{A}}\mathbf{W}\left(\beta^*\mathbf{C}_{xx|y}^{(l)} - \hat{\mathbf{x}}^{(l)}\mathbf{y}_s^H\right)\right\}\right\}, \quad (70)\end{aligned}$$

$$[\dot{\mathbf{A}}]_{p,q} = \begin{cases} 0, \text{ if } \left|p-q-\frac{f_d}{\Delta f}\right| = 0 \text{ or } M \\ \frac{j2\pi}{M^2\Delta f}\left[1-e^{j\frac{2\pi}{M}\left(\frac{f_d}{\Delta f}-p+q\right)}\right]^{-2}\left[e^{j\frac{2\pi}{M}\left(\frac{f_d}{\Delta f}-p+q\right)}+(M-1)\,e^{j\frac{2\pi(M+1)}{M}\left(\frac{f_d}{\Delta f}-p+q\right)}-Me^{j2\pi\left(\frac{f_d}{\Delta f}-p+q\right)}\right], \\ \qquad\qquad\qquad\qquad\qquad\qquad\qquad\qquad\qquad\qquad\qquad\qquad\qquad\qquad \text{otherwise} \end{cases}$$
$$\text{for } p,q=1,2,\ldots,M \tag{73}$$

$$[\ddot{\mathbf{A}}]_{p,q} = \begin{cases} 0, \text{ if } \left|p-q-\frac{f_d}{\Delta f}\right| = 0 \text{ or } M \\ \frac{4\pi^2}{M^3(\Delta f)^2}\left[1-e^{j\frac{2\pi}{M}\left(\frac{f_d}{\Delta f}-p+q\right)}\right]^{-3}\Big[(M-1)^2\,e^{j\frac{2\pi(M+2)}{M}\left(\frac{f_d}{\Delta f}-p+q\right)}-e^{j\frac{4\pi}{M}\left(\frac{f_d}{\Delta f}-p+q\right)}-e^{j\frac{2\pi}{M}\left(\frac{f_d}{\Delta f}-p+q\right)} \\ -(2M^2-2M-1)e^{j\frac{2\pi(M+1)}{M}\left(\frac{f_d}{\Delta f}-p+q\right)}+M^2e^{j2\pi\left(\frac{f_d}{\Delta f}-p+q\right)}\Big], \text{ otherwise} \end{cases}$$
$$\text{for } p,q=1,2,\ldots,M \tag{74}$$

and

$$\frac{\partial^2 Q_1\left(\boldsymbol{\theta};\hat{\boldsymbol{\theta}}^{(l)}\right)}{\partial f_d^2} = |\alpha|^2\mathrm{tr}\Big\{\mathbf{W}\mathbf{C}_{xx|y}^{(l)}\mathbf{W}^H\Big(\ddot{\mathbf{A}}^H\mathbf{C}_{ns}^{-1}\mathbf{A} + 2\dot{\mathbf{A}}^H\mathbf{C}_{ns}^{-1}\dot{\mathbf{A}} + \mathbf{A}^H\mathbf{C}_{ns}^{-1}\ddot{\mathbf{A}}\Big)\Big\} + 2\Re\Big\{\mathrm{tr}\Big\{\alpha\mathbf{C}_{ns}^{-1}\ddot{\mathbf{A}}\mathbf{W} \times\Big(\beta^*\mathbf{C}_{xx|y}^{(l)}-\hat{\mathbf{x}}^{(l)}\mathbf{y}_s^H\Big)\Big\}\Big\}, \tag{71}$$

with

$$\dot{\mathbf{A}} = \frac{\partial\mathbf{A}}{\partial f_d} \text{ and } \ddot{\mathbf{A}} = \frac{\partial^2\mathbf{A}}{\partial f_d^2}. \tag{72}$$

The entries of $\dot{\mathbf{A}}$ and $\ddot{\mathbf{A}}$ are shown in (73) and (74), at the top of the page, respectively.

Appendix C
Derivation of (27) and (28)

As the iterative process converges, we have: (i) $\hat{\tau}^{(l+1)} \approx \hat{\tau}^{(l)}$, (ii) $\hat{f}_d^{(l+1)} \approx \hat{f}_d^{(l)}$, and (iii) $\mathbf{C}_{xx|y}^{(l)} \approx \hat{\mathbf{x}}^{(l)}(\hat{\mathbf{x}}^{(l)})^H$. Thus, (21) and (22) can be approximated as

$$\begin{aligned}\left\{\hat{\tau}^{(l+1)},\hat{f}_d^{(l+1)}\right\} &\approx \arg\min_{\tau,f_d} Q_1\left(\tau,f_d,\hat{\alpha}^{(l)},\hat{\beta}^{(l)};\hat{\boldsymbol{\theta}}^{(l)}\right)\\ &\approx \arg\min_{\tau,f_d}\Gamma^{(l)}(\tau,f_d),\end{aligned} \tag{75}$$

where the first approximation is due to (i) and (ii), the second one is obtained by using (iii), and

$$\begin{aligned}&\Gamma^{(l)}(\tau,f_d)\\ &= 2\Re\left\{\hat{\alpha}^{(l)}(\hat{\beta}^{(l)}\hat{\mathbf{x}}^{(l)})^H\mathbf{C}_{ns}^{-1}\mathbf{A}\mathbf{W}\hat{\mathbf{x}}^{(l)}-\hat{\alpha}^{(l)}\mathbf{y}_s^H\mathbf{C}_{ns}^{-1}\mathbf{A}\mathbf{W}\hat{\mathbf{x}}^{(l)}\right\}\\ &\quad+|\hat{\alpha}^{(l)}|^2(\mathbf{A}\mathbf{W}\hat{\mathbf{x}}^{(l)})^H\mathbf{C}_{ns}^{-1}\mathbf{A}\mathbf{W}\hat{\mathbf{x}}^{(l)}\\ &= -2\Re\left\{\left[\mathbf{C}_{ns}^{-\frac{1}{2}}\left(\mathbf{y}_s-\hat{\beta}^{(l)}\hat{\mathbf{x}}^{(l)}\right)\right]^H\mathbf{C}_{ns}^{-\frac{1}{2}}\hat{\alpha}^{(l)}\mathbf{A}\mathbf{W}\hat{\mathbf{x}}^{(l)}\right\}\\ &\quad+\left\|\mathbf{C}_{ns}^{-\frac{1}{2}}\hat{\alpha}^{(l)}\mathbf{A}\mathbf{W}\hat{\mathbf{x}}^{(l)}\right\|^2\\ &= \left\|\mathbf{C}_{ns}^{-\frac{1}{2}}\left(\mathbf{y}_s-\hat{\beta}^{(l)}\hat{\mathbf{x}}^{(l)}-\hat{\alpha}^{(l)}\mathbf{A}\mathbf{W}\hat{\mathbf{x}}^{(l)}\right)\right\|^2\\ &\quad-\left\|\mathbf{C}_{ns}^{-\frac{1}{2}}\left(\mathbf{y}_s-\hat{\beta}^{(l)}\hat{\mathbf{x}}^{(l)}\right)\right\|^2.\end{aligned} \tag{76}$$

By ignoring the second term of the last equation in (76), which does not depend on τ and f_d, we obtain (28). When the disturbance in the SC is white Gaussian distributed with unit power, i.e., $\mathbf{C}_{ns}=\mathbf{I}_M$, (28) can be simplified as (27).

References

[1] H. D. Griffiths and C. J. Baker, "Passive coherent location radar systems. Part 1: Performance prediction," *IEE Proc. Radar Sonar Navig.*, vol. 152, no. 3, pp. 124–132, Jun. 2005.

[2] C. J. Baker, H. D. Griffiths, and I. Papoutsis, "Passive coherent location radar systems. Part 2: Waveform properties," *IEE Proc. Radar Sonar Navig.*, vol. 152, no. 3, pp. 160–168, Jun. 2005.

[3] P. E. Howland, D. Maksimiuk, and G. Reitsma, "FM radio based bistatic radar," *IEE Proc. Radar Sonar Navig.*, vol. 152, no. 3, pp. 107–115, Jun. 2005.

[4] M. K. Baczyk and M. Malanowski, "Reconstruction of the reference signal in DVB-T based passive radar," *Int. J. Electron. Telecommun.*, vol. 57, no. 1, pp. 43–48, Mar. 2011.

[5] M. Tobias and A. D. Lanterman, "A probability hypothesis density-based multitarget tracker using multiple bistatic range and velocity measurements," in *Proc. 36th Southeast. Symp. Syst. Theory*, 2004, pp. 205–209.

[6] B. A. Yocom, B. R. L. Cour, and T. W. Yudichak, "A Bayesian approach to passive sonar detection and tracking in the presence of interferers," *IEEE J. Ocean. Eng.*, vol. 36, no. 3, pp. 386–405, Jul. 2011.

[7] B. Artman, "Imaging passive seismic data," *Geophys.*, vol. 71, no. 4, pp. SI117–SI187, Jul. 2006.

[8] Q. He and R. S. Blum, "The significant gains from optimally processed multiple signals of opportunity and multiple receive stations in passive radar," *IEEE Signal Process. Lett.*, vol. 21, no. 2, pp. 180–184, Feb. 2014.

[9] C. Bongioanni, F. Colone, S. Bernardini, L. Lelli, A. Stavolo, and P. Lombardo, "Passive radar prototypes for multifrequency target detection," in *Proc. SPIE* , 2007, pp. 1–7.

[10] G. Cui, J. Liu, H. Li, and B. Himed, "Target detection for passive radar with noisy reference channel," in *Proc. IEEE Radar Conf.*, Cincinnati, OH, USA, May 2014, pp. 0144–0148.

[11] G. Cui, J. Liu, H. Li, and B. Himed, "Signal detection with noisy reference for passive sensing," *Signal Process. (Elsevier)*, vol. 108, pp. 389–399, Mar. 2015.

[12] D. E. Hack, L. K. Patton, B. Himed, and M. A. Saville, "Detection in passive MIMO radar networks," *IEEE Trans. Signal Process.*, vol. 62, no. 11, pp. 2999–3012, Jun. 2014.

[13] D. E. Hack, L. K. Patton, B. Himed, and M. A. Saville, "Centralized passive MIMO radar detection without direct-path reference signals," *IEEE Trans. Signal Process.*, vol. 62, no. 11, pp. 3013–3023, Jun. 2014.

[14] L. Wang and B. Yazici, "Passive imaging of moving targets using sparse distributed apertures," *SIAM J. Imag. Sci.*, vol. 5, no. 3, pp. 769–808, 2012.

[15] K. S. Bialkowski, I. V. L. Clarkson, and S. D. Howard, "Generalized canonical correlation for passive multistatic radar detection," in *Proc. IEEE Statist. Signal Process. Workshop (SSP)*, Jun. 2011, pp. 417–420.
[16] J. Liu, H. Li, and B. Himed, "Two target detection algorithms for passive multistatic radar," *IEEE Trans. Signal Process.*, vol. 62, no. 22, pp. 5930–5939, Nov. 2014.
[17] K. Polonen and V. Koivunen, "Detection of DVB-T2 control symbols in passive radar systems," in *Proc. IEEE 7th Sens. Array Multichannel Signal Process. Workshop (SAM)*, Hoboken, NJ, USA, Jun. 2012, pp. 309–312.
[18] G. Cui, H. Li, and B. Himed, "A correlation-based signal detection algorithm in passive radar with DVB-T2 emitter," in *Proc. 48th Asilomar Conf. on Signals, Syst., Comput.*, Pacific Grove, CA, USA, Nov. 2014.
[19] D. K. P. Tan, M. Lesturgie, H. Sun, and Y. Lu, "Target detection performance analysis for airborne passive bistatic radar," in *Proc. IEEE Int. Geosci. Remote Sens. Symp.*, Jul. 2010, pp. 3553–3556.
[20] R. Tao, H. Z. Wu, and T. Shan, "Direct-path suppression by spatial filtering in digital television terrestrial broadcasting-based passive radar," *IET Radar, Sonar Navig.*, vol. 4, no. 6, pp. 791–805, Dec. 2010.
[21] F. Colone, R. Cardinali, P. Lombardo, O. Crognale, A. Cosmi, A. Lauri, and T. Bucciarelli, "Space-time constant modulus algorithm for multipath removal on the reference signal exploited by passive bistatic radar," *IET Radar, Sonar Navig.*, vol. 3, no. 3, pp. 253–264, Jun. 2009.
[22] A. P. Dempster, N. M. Laird, and D. B. Rubin, "Maximum likelihood from incomplete data via the EM algorithm," *J. Royal Statist. Soc., Ser. B (Methodolog.)*, vol. 39, no. 1, pp. 1–38, 1977.
[23] A. Jakobsson, A. L. Swindlehurst, and P. Stoica, "Subspace-based estimation of time delays and Doppler shifts," *IEEE Trans. Signal Process.*, vol. 46, no. 9, pp. 2472–2483, Sep. 1998.
[24] P. P. Moghaddam, H. Amindavar, and R. L. Kirlin, "A new time-delay estimation in multipath," *IEEE Trans. Signal Process.*, vol. 51, no. 5, pp. 1129–1142, May 2003.
[25] M. Wax, "The joint estimation of differential delay, Doppler, and phase," *IEEE Trans. Inf. Theory*, vol. 28, no. 5, pp. 817–820, Sep. 1982.
[26] S. Stein, "Differential delay/Doppler ML estimation with unknown signals," *IEEE Trans. Signal Process.*, vol. 41, no. 8, pp. 2717–2719, Aug. 1993.
[27] A. V. Oppenheim, R. W. Schafer, and J. R. Buck, *Discrete-Time Signal Processing*, 2nd ed. Upper Saddle River, NJ, USA: Prentice-Hall, 1999.
[28] E. Conte, A. De Maio, and G. Ricci, "Recursive estimation of the covariance matrix of a compound-Gaussian process and its application to adaptive CFAR detection," *IEEE Trans. Signal Process.*, vol. 50, no. 8, pp. 1908–1915, Aug. 2002.
[29] D. Bauso and R. Pesenti, "Generalized person-by-person optimization in team problems with binary decisions," in *Proc. Amer. Contr. Conf.*, Seattle, WA, USA, Jun. 2008, pp. 717–722.
[30] S. M. Kay, *Fundamentals of Statistical Signal Processing: Estimation Theory*. Upper Saddle River, NJ, USA: Prentice-Hall, 1993.
[31] R. A. Horn and C. R. Johnson, *Matrix Analysis*. Cambridge, U.K.: Cambridge University Press, 1985.

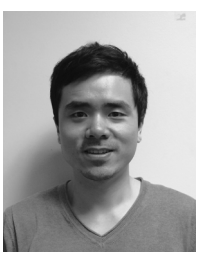

Xin Zhang received the B.Eng. degree (with honors) from the University of Science and Technology Beijing (USTB), China, in 2008, and the M.Eng. degree from Beijing University of Posts and Telecommunications (BUPT), in 2011, both in electrical engineering.

He is currently pursuing the Ph.D. degree in electrical engineering at Stevens Institute of Technology, Hoboken, NJ, USA, where he has been a Research and Teaching Assistant in the Department of Electrical and Computer Engineering since 2013. His research interests include statistical signal processing, optimization algorithms, passive sensing, and multichannel signal processing.

Hongbin Li (M'99–SM'08) received the B.S. and M.S. degrees from the University of Electronic Science and Technology of China, in 1991 and 1994, respectively, and the Ph.D. degree from the University of Florida, Gainesville, FL, USA, in 1999, all in electrical engineering.

From July 1996 to May 1999, he was a Research Assistant with the Department of Electrical and Computer Engineering, University of Florida. Since July 1999, he has been with the Department of Electrical and Computer Engineering, Stevens Institute of Technology, Hoboken, NJ, USA, where he became a Professor in 2010. He was a Summer Visiting Faculty Member at the Air Force Research Laboratory in the summers of 2003, 2004, and 2009. His general research interests include statistical signal processing, wireless communications, and radars.

Dr. Li received the IEEE Jack Neubauer Memorial Award in 2013 from the IEEE Vehicular Technology Soceity, the Outstanding Paper Award from the IEEE AFICON Conference in 2011, the Harvey N. Davis Teaching Award in 2003 and the Jess H. Davis Memorial Award for Excellence in Research in 2001 from Stevens Institute of Technology, and the Sigma Xi Graduate Research Award from the University of Florida in 1999. He has been a member of the IEEE SPS Signal Processing Theory and Methods Technical Committee (TC) and the IEEE SPS Sensor Array and Multichannel TC, an Associate Editor for *Signal Processing* (Elsevier), the IEEE TRANSACTIONS ON SIGNAL PROCESSING, IEEE SIGNAL PROCESSING LETTERS, and IEEE TRANSACTIONS ON WIRELESS COMMUNICATIONS, as well as a Guest Editor for IEEE JOURNAL OF SELECTED TOPICS IN SIGNAL PROCESSING and the EURASIP *Journal on Applied Signal Processing*. He has been involved in various conference organization activities, including serving as a General Co-Chair for the 7th IEEE Sensor Array and Multichannel Signal Processing (SAM) Workshop, Hoboken, NJ, June 17–20, 2012. He is a member of Tau Beta Pi and Phi Kappa Phi.

Jun Liu (S'11–M'13) received the B.S. degree in mathematics from Wuhan University of Technology, China, in 2006, the M.S. degree in mathematics from Chinese Academy of Sciences, China, in 2009, and the Ph.D. degree in electrical engineering from Xidian University, China, in 2012.

From July 2012 to December 2012, he was a Postdoctoral Research Associate with the Department of Electrical and Computer Engineering, Duke University, Durham, NC, USA. From January 2013 to September 2014, he was a Postdoctoral Research Associate with the Department of Electrical and Computer Engineering, Stevens Institute of Technology, Hoboken, NJ, USA. He is now with the National Laboratory of Radar Signal Processing, and also with Collaborative Innovation Center of Information Sensing and Understanding, both at Xidian University, where he is an Associate Professor. His research interests include statistical signal processing, optimization algorithms, passive sensing, and multistatic radar.

Braham Himed (S'88–M'90–SM'01–F'07) received the Engineer degree in electrical engineering from Ecole Nationale Polytechnique of Algiers in 1984, and the M.S. and Ph.D. degrees both in electrical engineering, from Syracuse University, Syracuse, NY, USA, in 1987 and 1990, respectively.

He is a Technical Advisor with the Air Force Research Laboratory, Sensors Directorate, RF Technology Branch, Dayton, OH, USA, where he is involved with several aspects of radar developments. His research interests include detection, estimation, multichannel adaptive signal processing, time series analyses, array processing, adaptive processing, waveform diversity, MIMO, passive radar, and over the horizon radar.

Dr. Himed is the recipient of the 2001 IEEE region I award for his work on bistatic radar systems, algorithm development, and phenomenology. He is the Vice-Chair of the AES Radar Systems Panel. He is the recipient of the 2012 IEEE Warren White award for Excellence in Radar Engineering. He is also a Fellow of AFRL (Class of 2013).